Chronic high-salt intake induces cardiomyocyte autophagic vacuolization during left ventricular maladaptive remodeling in spontaneously hypertensive rats

YING BI[1,2*], GUO-HONG YANG[2*], ZHAO-ZENG GUO[2], WEI CAI[2], SHAO-BO CHEN[2], XIN ZHOU[2,3*] and YU-MING LI[2,4]

[1]Department of Internal Medicine, Tianjin Corps Hospital of The Chinese People's Armed Police Forces, Tianjin 300163; [2]Institute of Prevention and Treatment of Cardiovascular Diseases in Alpine Environment of Plateau, Characteristic Medical Center of The Chinese People's Armed Police Forces, Tianjin 300162; [3]Department of Cardiovascular Diseases, General Hospital Tianjin Medical University, Tianjin 300052; [4]Department of Cardiovascular Diseases, TEDA International Cardiovascular Hospital, Tianjin 300457, P.R. China

Received September 29, 2022; Accepted January 27, 2023

DOI: 10.3892/etm.2023.11847

Abstract. The role of autophagy in high-salt (HS) intake associated hypertensive left ventricular (LV) remodeling remains unclear. The present study investigated the LV autophagic change and its association with the hypertensive LV remodeling induced by chronic HS intake in spontaneously hypertensive rats (SHR). Wistar Kyoto (WKY) rats and SHR were fed low-salt (LS; 0.5% NaCl) and HS (8.0% NaCl) diets and were subjected to invasive LV hemodynamic analysis after 8, 12 and 16 weeks of dietary intervention. Reverse transcription-quantitative PCR and western blot analysis were performed to investigate the expression of autophagy-associated key components. The LV morphologic staining was performed at the end of the study. The rat H9c2 ventricular myoblast cell-associated experiments were performed to explore the mechanism of HS induced autophagic change. A global autophagy-associated key component, as well as increased cardiomyocyte autophagic vacuolization, was observed after 12 weeks of HS intake. During this period, the heart from HS-diet-fed SHR exhibited a transition from compensated LV hypertrophy to decompensation, as shown by progressive impairment of LV function and interstitial fibrosis. Myocardial extracellular [Na^+] and the expression of tonicity-responsive enhancer binding protein (TonEBP) was significantly increased in HS-fed rats, indicating myocardial interstitial hypertonicity by chronic HS intake. The global autophagic change and overt deterioration of LV function were not observed in LS-fed SHR and HS-fed WKY rats. The study of rat H9c2 cardiomyocytes demonstrated a cytosolic [Na^+] elevation-mediated, reactive oxygen species-dependent the autophagic change occurred when exposed to an increased extracellular [Na^+]. The present findings demonstrated that a myocardial autophagic change participates in the maladaptive LV remodeling induced by chronic HS intake in SHR, which provides a possible target for future intervention studies on HS-induced hypertensive LV remodeling.

Correspondence to: Dr Xin Zhou, Department of Cardiovascular Diseases, General Hospital Tianjin Medical University, 154 An-Shan Road, Heping, Tianjin 300052, P.R. China
E-mail: xzhou@live.com

Dr Yu-Ming Li, Department of Cardiovascular Diseases, TEDA International Cardiovascular Hospital, 61 Third Avenue, TEDA, Tianjin 300457, P.R. China
E-mail: cardiolab@live.com

*Contributed equally

Abbreviations: HS, high salt; BP, blood pressure; ROS, reactive oxygen species; LV, left ventricular; TAC, transverse aortic constriction; SHR, spontaneously hypertensive rats; WKY, Wistar Kyoto rats; SBP, systolic blood pressure; DBP, diastolic blood pressure; LVEDP, LV end-diastolic pressure; H&E, hematoxylin and eosin; DAPI, 4,6-diamidino-2-phenylindole; AB-PAS, Alcian blue/periodic acid-Schiff; WW, wet weight; DW, dry weight; NAC, N-acetylcysteine; DCFH-DA, 2,7-dichlorofluorescein diacetate; FITC, fluorescein isothiocyanate; PI, propidium iodide; TonEBP, tonicity responsive enhancer binding protein

Key words: hypertension, heart failure, autophagy, oxidative stress, spontaneously hypertensive rat

Introduction

Chronic high-salt (HS) intake is closely associated with elevated blood pressure (BP) level and target organ injuries (1,2). In addition, ample evidence has demonstrated that excessive salt intake could also adversely affect cardiac functional and structural remodeling via BP-independent mechanisms (3,4). Previous studies showed that uncontrolled oxidative stress is a key pathophysiological process during the development of heart failure (5), presumably via reactive oxygen species (ROS)-mediated apoptosis, leading to cardiomyocyte loss, and ultimately, left ventricular (LV) dysfunction in murine

models (6,7). In response to chronic HS challenge, the heart initially manifests robust hypertrophic growth and interstitial fibrosis, followed by LV maladaptive remodeling, if stress persists. However, the exact mechanism governing the transition from compensated LV hypertrophy to a decompensated state during chronic HS challenge is not fully understood.

Autophagy is an essential, life-sustaining renewal process that involves the degradation of cell constituents, such as long-lived proteins and organelles, when subjected to cellular stress or during certain stages of development. Basal constitutive autophagy is indispensable for maintaining cellular homeostasis, whereas this process is upregulated in response to stressors, such as nutrient or growth factor deprivation, hypoxia and ischemia. In other settings, however, dysfunction in the autophagy pathway has been implicated in a range of pathological situations, such as neurodegenerative disorders, skeletal myopathy, cancer and infectious diseases (8).

Previously, alterations in autophagy activity have been implicated as a key pathological process in hypertensive LV remodeling and pressure overload (transverse aortic constriction; TAC) induced heart failure models (9-11). To the best of our knowledge, the autophagic change and its association with high-salt (HS) intake-accelerated progression of LV dysfunction has not been investigated. Therefore, the present study was designed to address this issue, as well as the potential molecular basis underlying this functional transition in HS-diet-fed spontaneously hypertensive rats (SHR). The present study would provide a novel mechanism to explain HS intake-induced cardiac remodeling.

Materials and methods

Animals. A total of seven-week-old male SHR and Wistar Kyoto rats (WKY) weighing 200-250 g were obtained from Shanghai Laboratory Animal Center of the Chinese Academy of Science (Shanghai, China), and received humane care in compliance with the Guide for the Care and Use of Laboratory Animals (NIH Pub. no. 85-23, revised 1996), which was approved by the Institutional Ethics Review Board of the Characteristic Medical Center of the Chinese People's Armed Police Forces (Tianjin, China; approval number: 2012-0005). Rats were maintained in a 12/12-h dark/light cycle in air-conditioned rooms (23±1˚C, 55±5% humidity) and were acclimated to the local conditions for 1 week before the study. At 8 weeks of age, rats were divided randomly (n=12 for each group), and then given either a low-salt (LS; 0.5% NaCl) or HS diet (8% NaCl) for 8, 12 or 16 weeks. All rats were permitted free access to chow and tap water.

Invasive hemodynamic measurements. A total of 8, 12 and 16 weeks after dietary intervention, the rats were anesthetized (sodium pentobarbital, 60 mg/kg, intraperitoneally) for invasive hemodynamics using a 2F high fidelity micro-tip pressure catheter (SPR-320; Millar Instruments Ltd.) to measure systolic and diastolic BP (SBP and DBP), LV end-diastolic pressure (LVEDP), maximal slope of systolic pressure increment ($+dP/dt_{max}$), and diastolic pressure decrement ($-dP/dt_{min}$) as previously described by the authors (12).

Cardiac pathological evaluation. Animals were euthanized with an overdose of sodium pentobarbital (100 mg/kg, intraperitoneally) after *in vivo* hemodynamic measurement, and then were rapidly perfused via inferior vena cava with precooled physiological saline for 5 min. The hearts were quickly removed, sectioned, and prepared for paraffin embedding and cryo-section. Routine staining techniques in paraffin embedded tissue (7-μm) included hematoxylin and eosin (H&E) staining (25˚C, 15 min) and Masson's trichrome staining for evaluating interstitial collagen deposition. Tetraethyl rhodamine isothiocyanate-conjugated wheat germ agglutinin (Invitrogen; Thermo Fisher Scientific, Inc.) plus 4,6-diamidino-2-phenylindole (DAPI; 5 mg/ml; Vector Laboratories, Inc.) staining was used to measure cardiomyocyte cross-sectional area, which was examined with a fluorescent microscope (80i; Nikon Corporation) as previously described by the authors (13). All image analysis was performed in a blinded manner by Image Pro Plus (version 4.5; Media Cybernetics, Inc.).

For detecting lipid droplet, Oil Red O staining was used in cryo-sectioned heart tissue (10 μm), and the sections were fixed with 10% buffered formalin (25˚C, 24 h) and stained with Oil Red O working solution (25˚C, 30 min). Hematoxylin was used for counterstaining. The perirenal adipose tissue was removed and smeared over a slide serving as the positive controls. For detecting sulfated proteoglycans, paraffin-embedded sections were stained with toluidine blue. Alcian blue/periodic acid-Schiff (AB-PAS) was used in paraffin-embedded sections to detect acidic sulfated mucins (AB positive), O-glycosides (PAS positive) and sialic acid (PAS positive) as previously described (14).

Transmission electron microscopy was performed for evaluating myocardial ultrastructure. Briefly, the samples from LV were fixed in 2.5% glutaraldehyde in 0.1 M phosphate buffer (pH 7.2; 4˚C, 24 h), post-fixed in 1.0% OsO4, dehydrated in alcohol and acetone solution, embedded in Epon812, sectioned with LKB ultramicrotome, and stained with uranyl acetate followed by lead citrate, then observed with a transmission electron microscope.

Cardiac tissue ashing procedure. A total of 8 weeks after dietary intervention, when LV hemodynamic measurement was finished, rat hearts were harvested. The blood was collected from superior vena cava for measurement of plasma [Na^+], [K^+] and [Cl^-]. The right ventricle was dissected away, and the left ventricle was weighted to determine the wet weight (WW). Then the hearts were desiccated at 90˚C for 72 h and their dry weights (DW) were determined. Because the weight was unchanged with further drying, the difference between WW and DW was considered as tissue water content. The tissues were then ashed at 200˚C, 400˚C for 24 h at each temperature level and 600˚C for a further 48 h and then were dissolved in 20 ml 10% HNO_3. [Na^+] and [K^+] were measured by inductively-coupled plasma emission spectrometer (ICP, IRIS Intrepid II XSP, Thermo Electron Corporation). [Cl^-] was measured by titration with 0.1 N silver nitrate (15).

Cell culture and treatments. H9c2, a rat ventricular myoblast cell line (Shanghai Cell Bank, Chinese Academy of Science) was maintained at 37˚C and 5% CO_2 in Dulbecco's modified Eagle's medium (HyClone; Cytiva) supplemented with 10% fetal bovine serum (FBS; Gibco; Thermo Fisher Scientific,

Table I. Primers used for reverse transcription-quantitative PCR analysis.

Primer name	Sequence (5'-3')	Product length (bp)	Tm (˚C)
β-actin	F: TCTGTGTGGATTGGTGGCTCT R: AGAAGCATTTGCGGTGCAC	115	60
Beclin1	F: CTCCTGTGGAATGGAATGA R: ACAACGGCAACTCCTTAG	168	49
LC3b	F: AAGGCTGAAGTCCAAGTG R: GAAGTGGCTGTATGTCTGT	192	50
ATG9A	F: GGCAGAAGAGATGGCAGGACAG R: TGGGAGGATGGGCAGAAGATGG	170	57
ATG16L1	F: TGGACAGTAGGAACAGACA R: CAGCGAATGACAGGTGAG	86	50

ATG, autophagy-related genes; LC3, light chain 3

Inc.) and 1% glutamine. H9c2 cells were seeded onto six-well plates and incubated with culture media containing NaCl (50 mM) or mannitol (100 mM), which yielded hypertonic state, equaling 400 mOsm/l, and treated with or without ROS scavenger N-acetylcysteine (NAC; 0.5 and 2 mM). Normal culture medium (isotonic, 300 mOsm/l) served as the control for the experiment. After exposure for desired time periods, the monolayer cultures were washed with D-Hanks and the cells were removed by 0.25% trypsin.

Measurement of apoptosis, intracellular free [Na^+] and ROS in H9c2 cells. Intracellular free Na^+ concentration ([Na^+]) was detected using the dye CoroNa™ Green (cat. no. C36676; Invitrogen; excitation 488 nm, emission at 516 nm) as previously described (16). Briefly, the H9c2 cells were cultured in six-well plates and treated with a NaCl concentration gradient (final concentrations were 25, 50, 100 and 150 mmol/l) for 24 h; after adding CoroNa Green (5 μmol/l), the fluorescence signal was detected by flow cytometry (Cytomic FC500; Beckman-Coulter, Inc.) and analyzed by FlowJo software (version 7.6.1; TreeStar Inc.).

ROS production was detected using the dye 2,7-dichlorofluorescein diacetate (DCFH-DA; MilliporeSigma). The H9c2 cells were pretreated with or without ROS scavenger NAC (0.5, 2 mM) for 1 h followed by incubation with NaCl (50 mM), mannitol (100 mM) or control medium for 90 min. Cells were removed by 0.25% trypsin with culture medium without FBS. DCFH-DA (10 μmol/l) was added to the H9c2 cells and incubated at 37˚C for 30 min in dark. Analysis of apoptosis was performed by an Annexin V-fluorescein isothiocyanate (FITC)/Propidium Iodide (PI) staining kit (BioLegend, Inc.). Briefly, H9c2 cells were seeded onto six-well plates and incubated with increased medium mannitol (100 mM), NaCl (50 mM) and NaCl (50 mM) supplemented with ROS scavenger NAC (0.5, 2 mM) for 24 h. Thereafter, the cells were harvested and washed twice with D-Hanks, centrifuged (4˚C, 350 x g, 5 min) and added 1X binding buffer (500 μl), Annexin V-FITC (2.5 μl) and PI (5 μl), incubated at room temperature in dark for 15 min then filtrated and kept on ice for an immediate detection by a FC500 flow cytometer.

Detection of autophagosomes in H9c2 cells. H9c2 cells were washed and fixed with 4% paraformaldehyde at 20˚C for 15 min. Then the cells were blocked in fetal bovine serum for 20 min and stained with primary antibodies against LC3 (1:500; cat. no. NB100-2220; Novus Biologicals, LLC) for 2 h at 37˚C. After washing four times with PBS for 5 min, cells were incubated with rhodamine red-conjugated secondary antibodies (1:100; cat. no. CW0161; Beijing Kangwei Century Biotechnology Co., Ltd.) for 1 h at 37˚C and the nuclei were counterstained with DAPI (1:100, Vector Laboratories, Inc.) for 20 min. Then images were examined with a fluorescent microscope (80i; Nikon Corporation). The median fluorescence intensity of LC3 positive area was determined by Image Pro Plus software (version 4.5; Media Cybernetics, Inc.).

RNA extraction and reverse transcription-quantitative (RT-q) PCR. Total RNA was extracted using TRIzol® reagent (Invitrogen; Thermo Fisher Scientific, Inc.) following the manufacturer's protocol. Briefly, the H9c2 cells were washed twice with D-Hanks and lysed with 1 ml of TRIzol®. Subsequently, total RNA was extracted by adding chloroform and subsequent centrifugation (4˚C, 12,000 x g, 5 min) and precipitation with isopropyl alcohol. The RNA concentration and purity were measured by NanoDrop 2000C (Thermo Fisher Scientific, Inc.) and the ration of optical density value (260/280 nm) was at 1.8 to 2.0. Total RNA (2 μg) was reverse-transcribed into cDNA using a reverse transcription kit (Promega Corporation) in 25-μl reaction volumes according to the manufacturer's instructions. Transcript expression levels were quantified by SYBR Green RT-qPCR using an ABI PRISM 7300 sequence detector system (Applied Biosystems; Thermo Fisher Scientific, Inc.). Primers used for PCR analysis are shown in Table I. The conditions for amplification were as follows: 95˚C for 10 min, followed by 40 cycles at 95˚C for 15 sec and 60˚C for 60 sec. The relative expression levels were calculated using the $2^{-\Delta\Delta Cq}$ method (17).

Protein extraction and western blot analysis. For *in vivo* experiments, the heart tissue was homogenized in the RIPA lysis buffer containing 50 mM Tris (pH 7.4), 150 mM NaCl, 1% Triton X-100, 1% sodium deoxycholate, 0.1% SDS, with

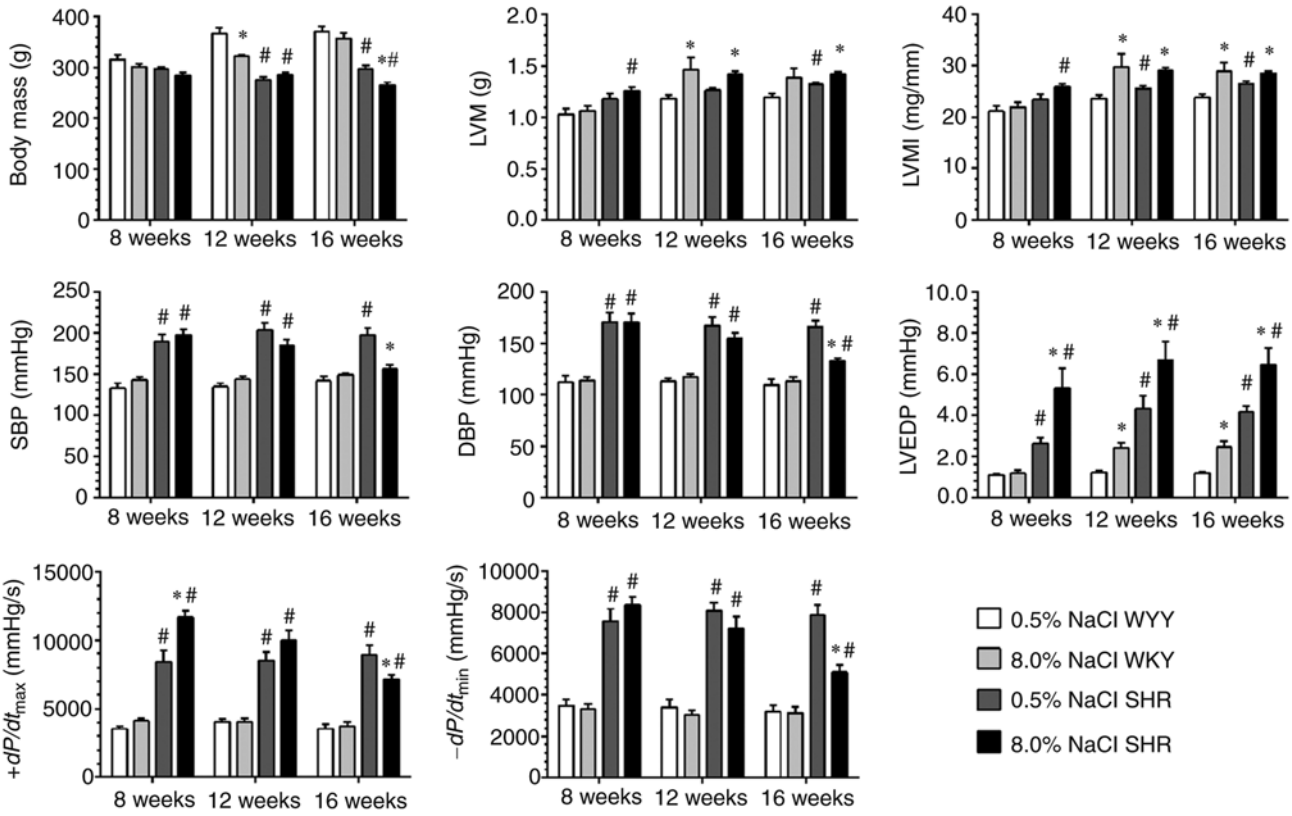

Figure 1. Dynamic changes in the rat body and LV mass and invasive hemodynamics during dietary intervention (n=8 each group). The statistical analysis of present data is determined by one-way ANOVA followed by Newman-Keuls post hoc test. *P<0.05 vs. 0.5% salt diet of the same strain at the same time point and #P<0.05 vs. WKY fed with the same salt diet at the same time point. LV, left ventricular; LVM, LV mass; LVMI, LV mass index; SBP, systolic blood pressure; DBP, diastolic blood pressure; LVEDP, LV end-diastolic pressure; $+dP/dt_{max}$ and $-dP/dt_{min}$, maximal rates of LV pressure rise and decline, respectively.

PMSF (100:1), incubated on ice for 30 min to obtain the whole-cell protein extraction, followed by centrifugation at 4˚C and 12,000 x g for 10 min. For *in vitro* examinations, the H9c2 cells were washed and centrifuged then lysed in RIPA buffer for 30 min on ice to obtain the protein extraction. The protein concentration was determined with BCA protein assay kit (Thermo Fisher Scientific, Inc.), following the manufacturer's instructions with bovine serum albumin (Gibco; Thermo Fisher Scientific, Inc.) as the standard. For western blotting, equal amounts of protein samples (50 μg) were added denaturing buffer and subjected to a 10 min boil at 99.5˚C. Following SDS-PAGE on 10 or 15% polyacrylamide gels, proteins were transferred onto PVDF membranes using the Trans-Blot Turbo blotting system (Bio-Rad Laboratories, Inc.) and incubated in 5% skim milk in PBST (PBS containing 0.1% v/v Tween 20) for 2 h at 37˚C, then respectively probed with primary antibodies against lysosome-associated membrane protein 1 (LAMP1; 1:1,000; cat. no. sc-17768; Santa Cruz Biotechnology, Inc.), light chain 3LC3; 1:1,000; cat. no. NB100-2220), autophagy-related gene (ATG) 9 (1:1,000; cat. no. NB110-56893), ATG5 (1:500; cat. no. NB110-53818), Beclin1 (1:8,000; cat. no. NB110-87318), ATG16L1 (1:1,000; cat. no. NB110-60928; all from Novus Biologicals, LLC), GAPDH (1:2,000; cat. no. ab181602; Abcam) at 4˚C overnight. After washing four times with PBST for 15 min, membranes were incubated with horseradish peroxidase-conjugated secondary antibodies (goat anti-rabbit IgG, cat. no. 6721, 1:2,000; goat anti-mouse IgG, cat. no. 6789, 1:2,000; Abcam) for 40 min at 37˚C. After washing fourth with PBST for 15 min, protein signals were detected by enhanced chemiluminescence method. The protein signal was amplified with Western Chemiluminescent Horseradish Peroxidase Substrate (MilliporeSigma) and detected using a Chemi DOC XRS+ Imaging System (Bio-Rad Laboratories, Inc.). Densitometric analyses were performed with Image J software (version 1.41o; National Institutes of Health).

Statistical analysis. All data are presented as the mean ± SEM. Statistical analysis was determined by independent sample unpaired t-test or one-way analysis of variance (ANOVA) followed by Newman-Keuls post hoc test using the GraphPad Prism v5 (GraphPad Prism Software Inc.). Two-tailed P<0.05 was considered to indicate a statistically significant difference.

Results

Transition from compensated LV hypertrophy to decompensation during HS intake in SHR. Body mass was comparable among all of the groups after 8 weeks of dietary intervention (Fig. 1). Throughout the 16 weeks of dietary intervention, there was a significant decrease in body weight in the SHR fed with the HS diet, which indicates a deteriorating health status. Moreover, the HS diet also led to an increase in LV mass, cardiomyocyte hypertrophy and collagen deposition in SHR and WKY compared with their LS-diet-fed counterparts (Figs. 1 and 2). Invasive LV hemodynamic analysis revealed

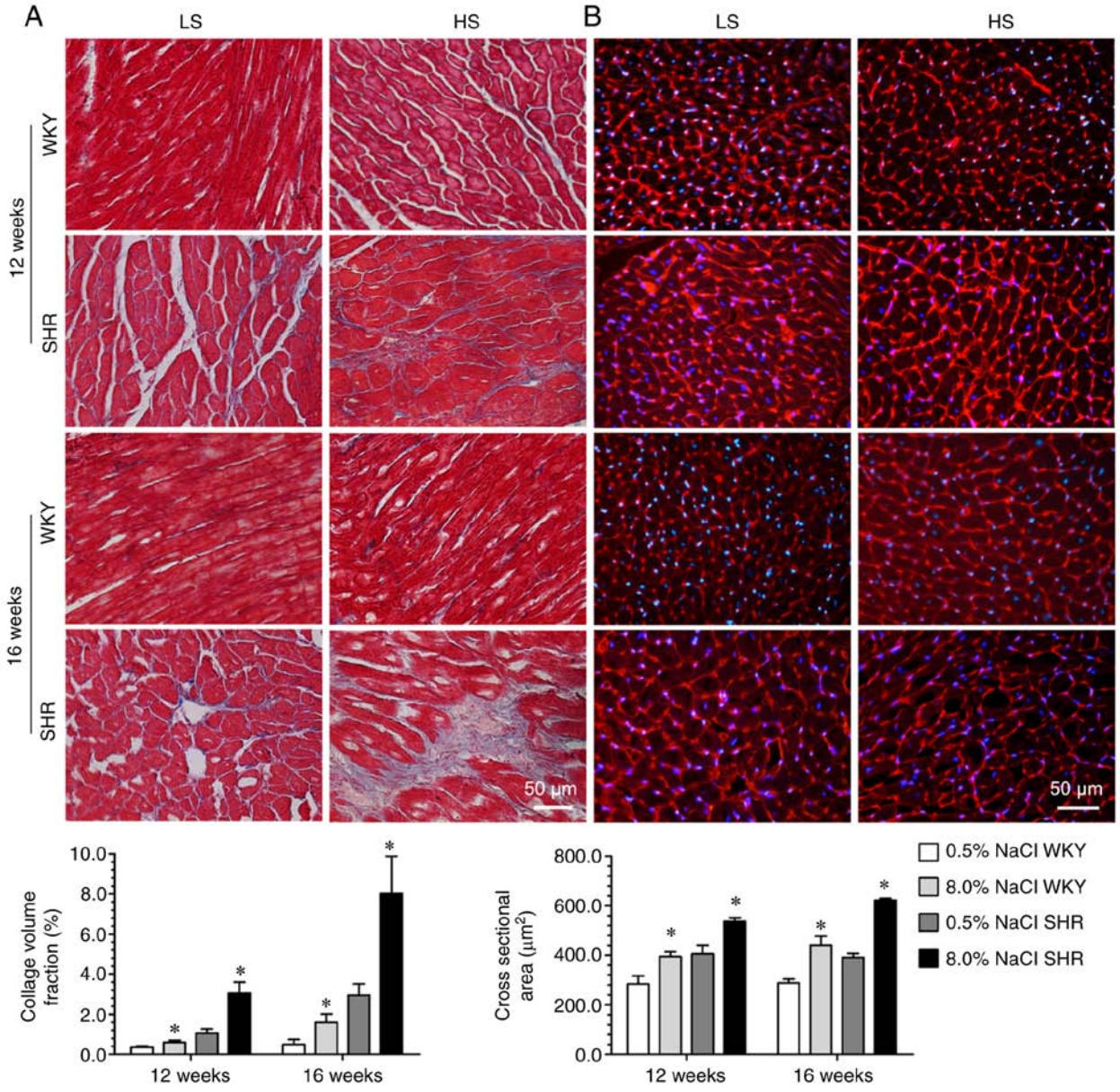

Figure 2. Collagen deposition and myocardial hypertrophy during dietary intervention. (A) Representative images using Masson's trichrome staining to reveal myocardial collagen desorption. (B) Representative tetraethyl rhodamine isothiocyanate-conjugated wheat germ agglutinin plus 4,6-diamidino-2-phenylindole staining for visualization of cardiomyocyte cross sectional area. Scale bar, 50 μm. The statistical analysis of present data is determined by one-way ANOVA followed by Newman-Keuls post hoc test. *P<0.05 vs. 0.5% salt diet of same strain. LS, low-salt (0.5% NaCl); HS, high salt (8.0% NaCl). WKY, Wistar Kyoto rats; SHR, spontaneously hypertensive rats.

that the HS diet progressively impaired the LV systolic (SBP and $+dp/dt_{max}$) and diastolic (LVEDP and $-dp/dt_{min}$) functions of the SHR in a time-dependent manner (Fig. 1). These results demonstrated that a transition from compensated LV hypertrophy to decompensation occurred when the HS diet intervention persisted for 12 weeks in the SHR. A time-dependent increase in collagen deposition and LVEDP was also noted in the LS-fed SHR and HS-fed WKY rats, but an obvious deterioration of the LV systolic and diastolic functions was not observed during this period in these two groups (Figs. 1 and 2).

Chronic HS Intake induces myocardial autophagic vacuolization in SHR. After 12 weeks of dietary intervention, massive vacuole-like structures were observed in LV tissue from HS-diet-fed SHR, compared with LS-diet-fed SHR (Fig. 3A and B). To examine the potential reasons accounting for these structures, various staining methods and TEM were performed for pathological examinations (Fig. 3). The results showed that these cardiac vacuoles observed in the HS-fed SHR under light microscopy are due to autophagic vacuolization (double-membrane vesicles containing cytoplasmic organelles). Depending on the engulfed structures (from protein aggregates, intracellular organelles to pathogens), the size of the autophagosomes can range from 0.5 to 10 μm in diameter (18). As revealed in Fig. 3, the size of these vacuole-like structures, observed under light microscopy, could be even larger than 20 μm in diameter; this finding has previously been reported in humans (19), and may be due to the fusion of the autophagosomes.

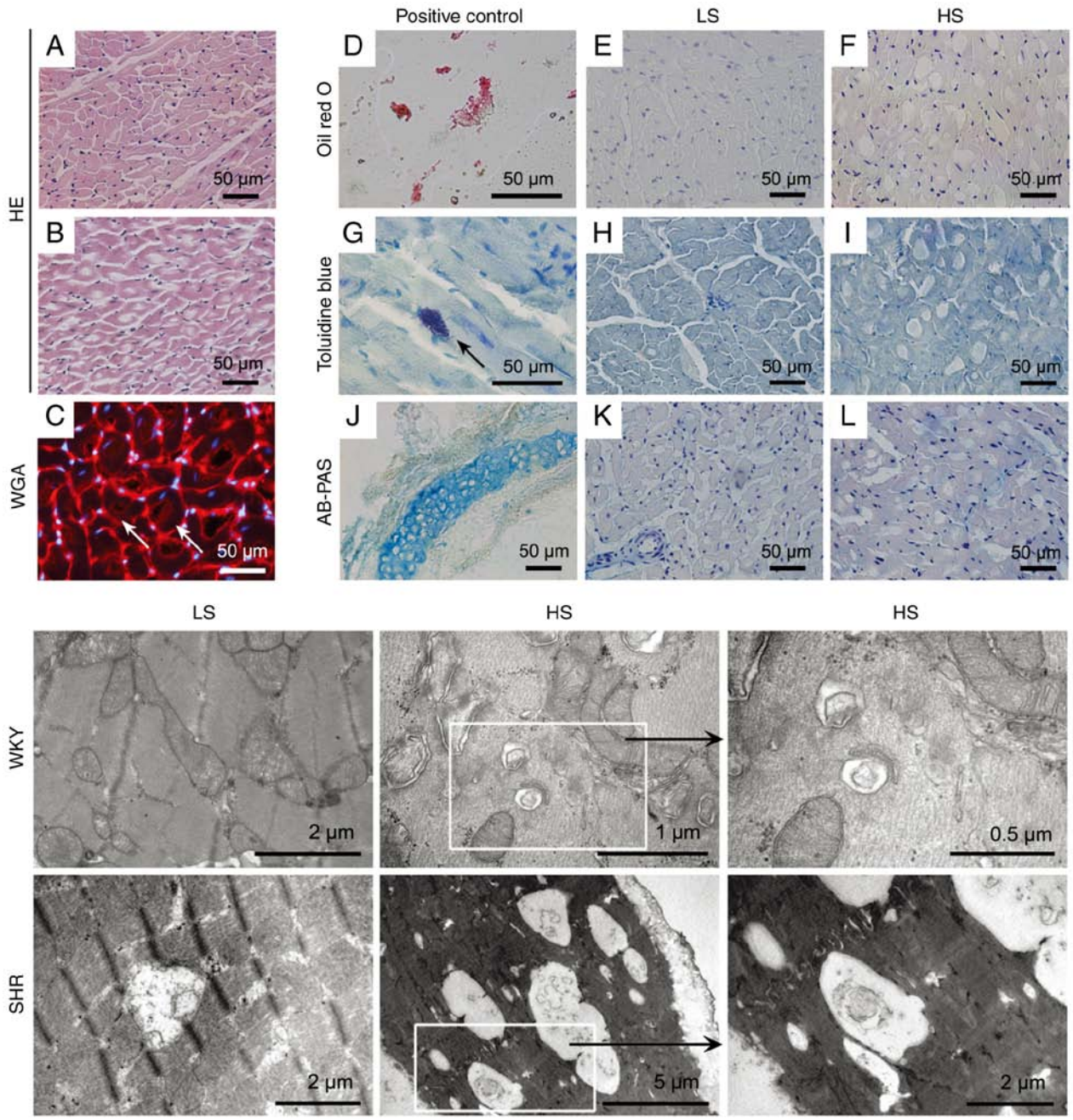

Figure 3. Pathological evaluation of cardiac vacuoles induced by HS intake using different staining methods (upper panel) and transmission electron microscopy (lower panel). (A and B) H&E staining of representative heart sections from LS- (A, 0.5% NaCl) and HS- (B, 8.0% NaCl) fed SHR for 12 weeks, respectively. (C) A heart section from HS- (B, 8.0% NaCl) fed SHR using wheat germ agglutinin conjugated by tetraethyl rhodamine isothiocyanate (red) to reveal the cell membrane (the nuclei were counterstained by 4'-6-diamidino-2-phenylindole, blue). The arrows indicate that these vacuole-like structures are inside the cardiomyocytes. (D-F) Oil red O staining revealed that these cardiac vacuoles are not fatty droplets (D: rat abdominal adipose tissue smearing was used as the positive controls.) (G-I) Toluidine blue staining revealed that the vacuoles are also negative for glycosaminoglycan. (G) shows a typical interstitial mast cell (arrow) positive for toluidine blue. (J-L) AB-PAS staining, which is used to detect acidic sulfated mucins (AB), O-glycosides (PAS) and sialic acid (PAS), was also negative for cardiac vacuoles. (J) The rat tracheal cartilage (AB-PAS positive, blue) was used as the positive control. Scale bars in the upper panel indicate 50 μm. The lower panel shows representative transmission electron microscopic images from LS- and HS-fed rats after 12 weeks of dietary intervention. There are numerous double-membrane vesicles containing cytoplasmic organelles characteristic of autophagy, particularly in the HS-fed SHR. HS, high-salt; LS, low-salt; WKY, Wistar Kyoto rats; SHR, spontaneously hypertensive rats. Alcian blue/periodic acid-Schiff.

A time-dependent of cardiac autophagic change accompanies LV functional deterioration in SHR during HS Intake. Next, autophagy-associated key proteins in LV tissue from SHR sacrificed at different time points were examined by western blotting (Fig. 4). The results demonstrated a global change of the autophagy since SHR was fed by HS diet for 12 weeks. This change persisted to 16 weeks in SHR on the HS diet, as shown by upregulated Beclin 1/ATG6 (required for autophagy induction and nucleation), ATG16-ATG5-ATG12 and LC3-II (two complexes required for phagophore formation and autophagosome expansion), LAMP1 (maker for lysosome fusion with the autophagosome to form an autolysosome) and ATG9 (necessary for most ATG protein recycle). These results clearly demonstrated a

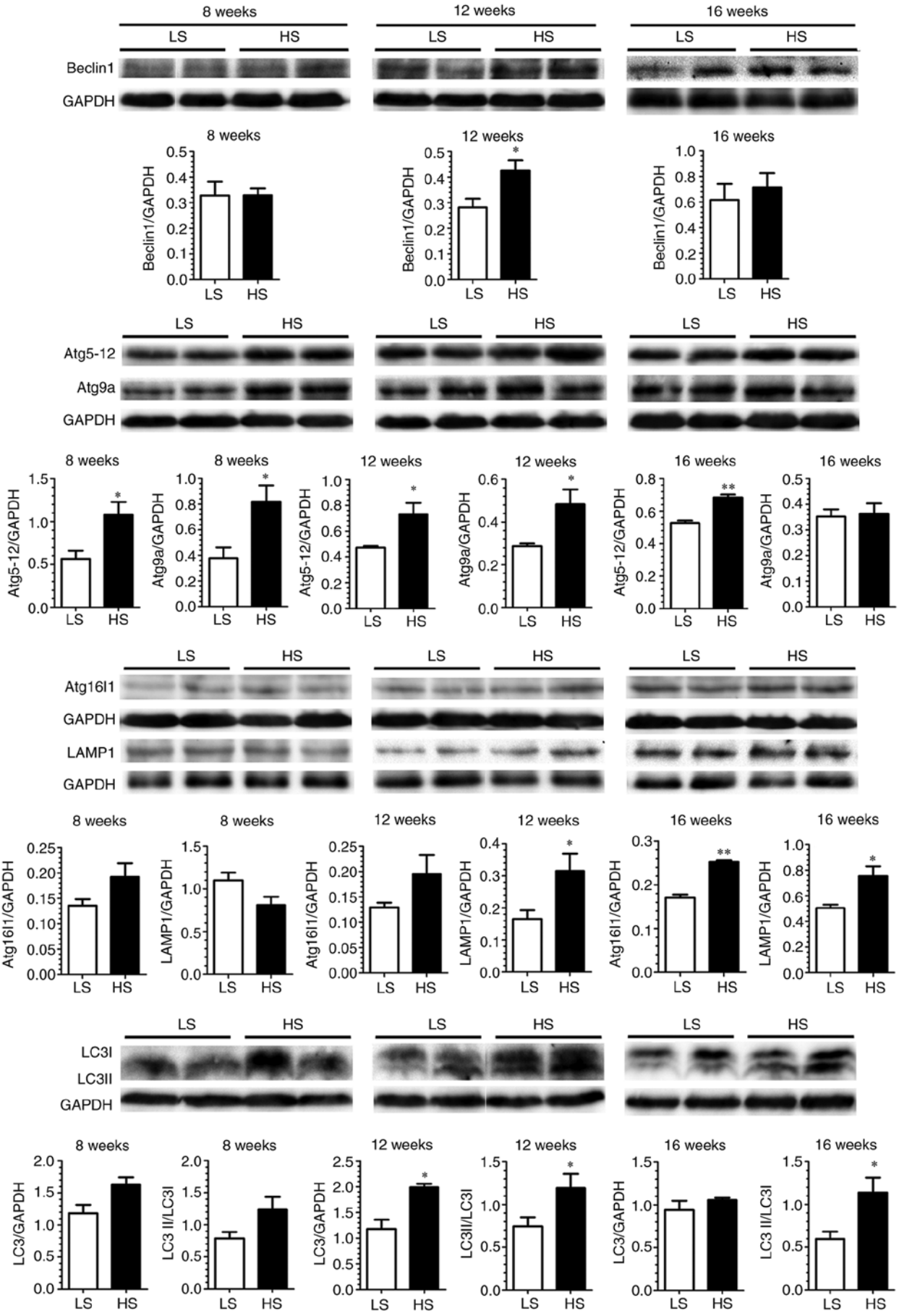

Figure 4. Global upregulation of autophagy related proteins in myocardium of spontaneously hypertensive rats after HS- (8.0% NaCl) loading compared with LS- (0.5% NaCl) fed SHR. *P<0.05 and **P<0.01. The statistical results are derived from 4 to 5 independent tests. HS, high-salt; LS, low-salt; ATG, autophagy-related genes; LC3, light chain 3; LAMP1, lysosome-associated membrane protein 1.

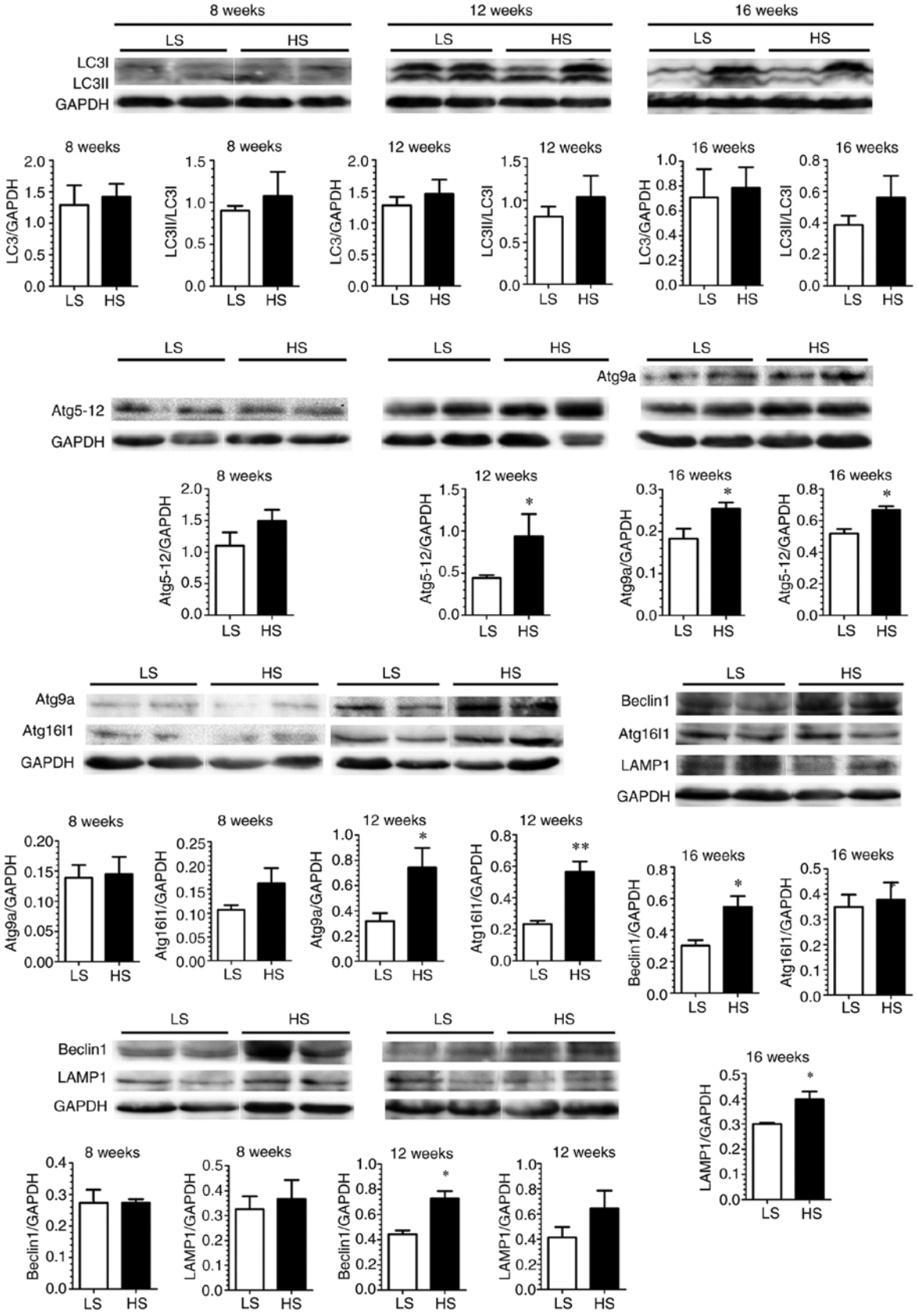

Figure 5. Western blot analysis of autophagy-related proteins in WKY myocardium after HS (8.0% NaCl) loading compared with LS (0.5% NaCl) fed WKY. $^{*}P<0.05$ and $^{**}P<0.01$. The statistical results are derived from 4 to 5 independent tests. WKY, Wistar Kyoto rats; HS, high-salt; LS, low-salt; ATG, autophagy-related genes; LC3, light chain 3; LAMP1, lysosome-associated membrane protein 1.

temporal and spatial association between autophagic change and LV function deterioration in the HS-fed SHR. Similarly, but to a lesser extent (not global), autophagic change was observed in the HS-fed WKY (Fig. 5).

Na^+ leak-induced cytosolic [Na^+] elevation contributes to ROS-dependent autophagic change in H9c2 Cardiomyocytes. Increasing evidence shows that chronic HS intake could induce Na^+ accumulation in the interstitial space without a commensurate retention of water, which yields increased tonicity (18,20,21). As shown in Fig. 6, upregulation of myocardial TonEBP was also demonstrated in the HS-fed WKY and SHR. In addition, using LV ashing samples, LV tissue composition analysis of Na^+, K^+ and water was performed in SHR after dietary intervention for 8 weeks. The results revealed that cardiac extracellular [Na^+] was markedly higher than plasma level (215.0±2.0 mmol/l vs. 139.1±1.84 mmol/l) in LS-diet-fed SHR, and this difference was further increased in HS-diet-fed SHR (237.0±6.0 mmol/l, Table II). To examine the impact of increased extracellular [Na^+] on the autophagic response in rat H9c2 cardiomyocytes, an additional NaCl concentration gradient was added in the culture medium. It was identified that there was a proportional increase of cytosolic [Na^+] as extracellular [Na^+] increased (Fig. 7A), indicating a Na^+ leak into the cytosol when the cells were exposed to high [Na^+]. A previous study showed that HS loading with a diet containing 8.0% NaCl in Sprague-Dawley rats for 2 weeks led to an increase of [Na^+] ~40 mM in the skin compared with serum [Na^+] (15). Based on the relationship between extracellular and intracellular [Na^+] in H9c2 cells and cardiac extracellular [Na^+] (Fig. 7A and Table II), an additional 50 mM NaCl was thus used in the culture medium, which equals 400 mOsm/l (serum osmolality is ~300 mOsm/l), to simulate the extracellular hyperosmolarity induced by chronic HS intake in the subsequent *in vitro* studies. It was found that incubation with an additional 50 mM NaCl induced an upregulation of key components of autophagy at both the mRNA and protein levels (Fig. 7B and C).

In addition, it was identified that the exposure of H9c2 cells to an additional 50 mM NaCl in the culture medium led to an enhanced intracellular ROS production (Fig. 8A), as well as increased pro-apoptotic response (Fig. 8B). When NAC was used as a ROS scavenger, the high NaCl-induced upregulation of pro-apoptotic response was significantly attenuated (Fig. 8B). Similarly, when exposure to the high extracellular NaCl occurred, there was an upregulation of key autophagy components both at mRNA and protein levels, as well as increased autophagosome formation (Fig. 9), which could be suppressed by NAC, implying that high [Na^+]-induced autophagic change is ROS-dependent. Notably, when 100 mM mannitol (400 mOsm/l) was used as a positive control at the same extracellular hyperosmolality with 50 mM NaCl, the magnitude of ROS generation (Fig. 8) and the pattern of key autophagic component upregulation were different from those achieved by 50 mM NaCl, providing evidence to indicate that high [Na^+]-induced changes in H9c2 cells are not entirely dependent on extracellular osmolality (Fig. 9A-D).

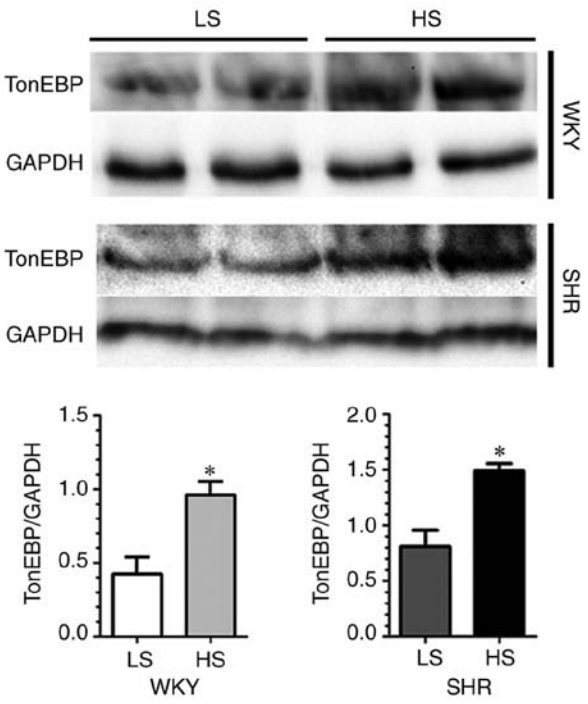

Figure 6. Myocardial TonEBP is upregulated in the HS (8.0% NaCl) group compared with the LS (0.5% NaCl) fed rats. *P<0.05. The statistical results are derived from 4 independent tests. TonEBP, tonicity-responsive enhancer binding protein; HS, high-salt; LS, low-salt.

Discussion

In the present study, for the first time, it was demonstrated that chronic dietary HS intake could induce LV autophagic change and myocardial autophagic vacuolization in SHR. More importantly, there is a temporal coincidence between the transition from compensated to decompensated LV hypertrophy and cardiomyocyte autophagic change, which indicates an important role of the myocardial autophagy during the development of hypertensive heart remodeling. In addition, it was showed that chronic HS intake-induced myocardial interstitial hypertonicity, the majority of which is harbored by Na^+, via a Na^+ leak-induced cytosolic [Na^+] elevation, contributes to autophagic change in cardiomyocytes in a ROS-dependent manner.

Cardiomyocyte vacuolization is a common pathological finding observed in a variety of pathological conditions, including hypertrophic cardiomyopathy (22), idiopathic dilated cardiomyopathy (19), arrhythmogenic right ventricular cardiomyopathy/dysplasia (23), and chronic and acute coronary ischemia (24). The content inside these intracellular vacuole-like structures is quite different depending on the underlying pathological mechanisms. Nonetheless, the existence of myocardial vacuolization is a sign of worsening LV function, and is associated with poor prognosis (25). In the present study, it was found that there are more vacuoles in HS-loaded SHR compared with their LS-diet-fed counterparts or WKY rats, indicating a HS intake-related phenomenon. After careful investigations by different staining methods and TEM examination, these cardiac vacuoles observed in the HS-fed SHR under light microscopy were proven to be autophagic vacuolization.

Previously, autophagy has been implicated as a key process during hypertension-related heart disease, whose impact on LV remodeling is determined by three factors, i.e., basal autophagy level, stress severity and duration (26). The importance of basal autophagic activity has been well defined by *Atg*-modified mice. Zhu *et al* (27) demonstrated that the partial suppression of autophagy using *Beclin 1*$^{+/-}$ mice blunted

Table II. Electrolytes and water distribution in plasma and heart tissue of SHR.

Electrolytes and water distribution indexes	Low-salt diet	High-salt diet
Plasma [Na^+] (mmol/l)	139.1±1.84	141.1±0.92
Plasma [K^+] (mmol/l)	4.17±0.21	3.94±0.18
Cardiac muscle water (ml/g DW)	3.526±0.020	3.700±0.057[a]
Cardiac muscle K^+/cardiac muscle water (mmol/ml)	0.075±0.002	0.063±0.005[a]
Cardiac muscle Na^+/cardiac muscle water (mmol/ml)	0.102±0.002	0.135±0.007[a]
Cardiac muscle K^+ (mmol/g DW)	0.265±0.008	0.231±0.017
Cardiac muscle Na^+ (mmol/g DW)	0.359±0.006	0.499±0.034[a]
Cardiac muscle extracellular fluid (ml/g WW)	0.370±0.011	0.448±0.027[a]
Cardiac muscle intracellular fluid (ml/g WW)	0.409±0.011	0.339±0.026[a]
Cardiac muscle Na^+/cardiac muscle extracellular fluid (mmol/ml)	0.215±0.002	0.237±0.006[a]

[a]P<0.05 vs. LS diet, n=5 in each group; values are expressed as the mean ± SEM. DW, dry weight; WW, wet weight; HS, high salt; LS, low salt.

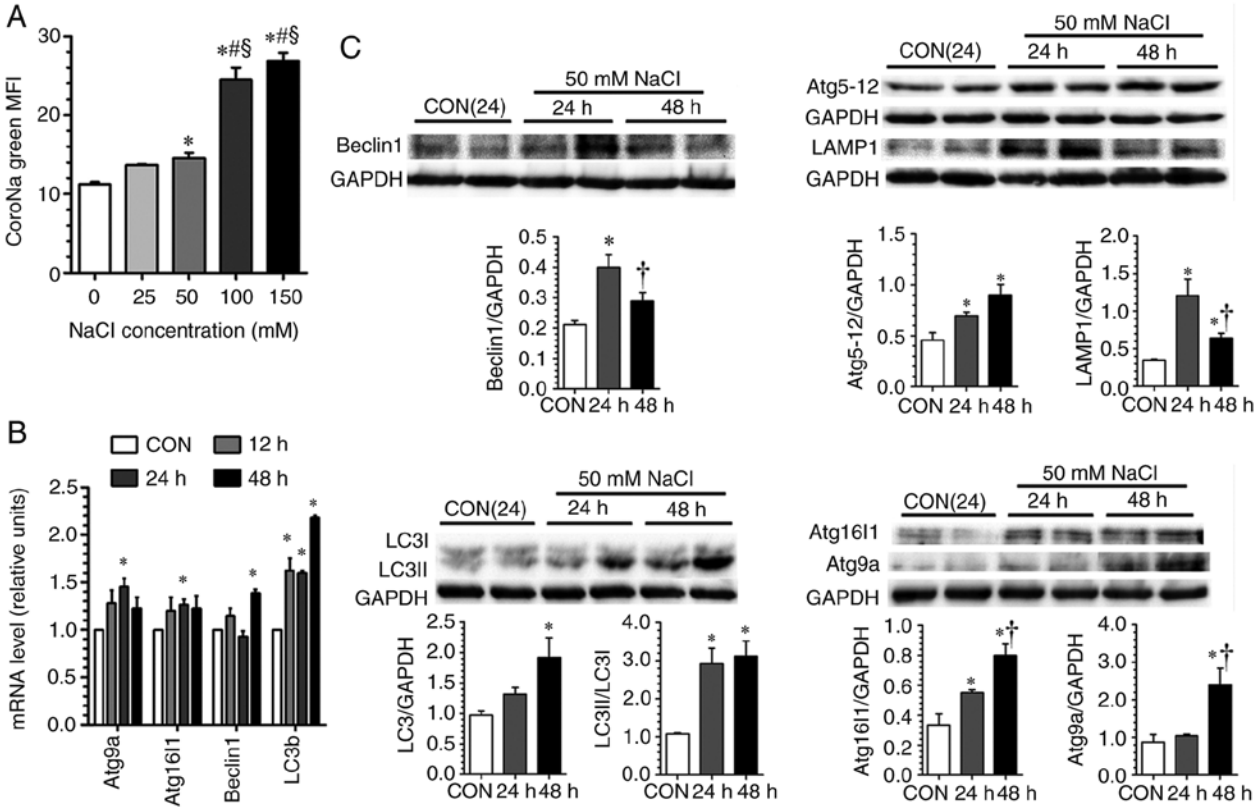

Figure 7. Increased extracellular [Na^+] contributes to elevation in cytosolic [Na^+] and upregulation of autophagy related proteins in H9c2 cells. (A) Changes in cytosolic [Na^+] determined by flow cytometry using CoroNa green™ as a sodium dye after exposure to a NaCl concentration gradient in the culture medium. (B) Reverse transcription-quantitative PCR analysis of mRNA levels of key autophagy-related genes in H9c2 cells after treatment with or without 50 mM NaCl in the culture medium for 12, 24 and 48 h. (C) Western blot analysis of key autophagy-related proteins in the H9c2 cells after treatment with or without 50 mM NaCl in the culture medium for 24 and 48 h. The statistical analysis of present data is determined by one-way ANOVA followed by Newman-Keuls post hoc test. *P<0.05 vs. control (no additional NaCl), #P<0.05 vs. 25 mM NaCl and §P<0.05 vs. 50 mM NaCl; †P<0.05 vs. 50 mM NaCl for 24 h. The statistical results are derived from 4 to 5 independent tests. CON, control group (no additional NaCl); MFI, median fluorescence intensity; ATG, autophagy-related genes; LC3, light chain 3.

pressure overload TAC-induced LV adverse remodeling (27). Conversely, *Beclin 1* overexpression accentuated load-induced LV pathological remodeling (27). Another study using an *Atg5* loss-of-function mice, in which constitutive autophagy is near-completely inactivated, demonstrated a deterioration of LV function in a TAC model (28). These lines of evidence support the notion that, in the basal state, constitutive levels of autophagy are required for cell survival, while the uncontrolled activation of autophagy during sustained stress eliminates essential cellular elements and provokes cell death (26).

In terms of the roles of stress severity and duration in initiating myocardial autophagy, the present model could provide

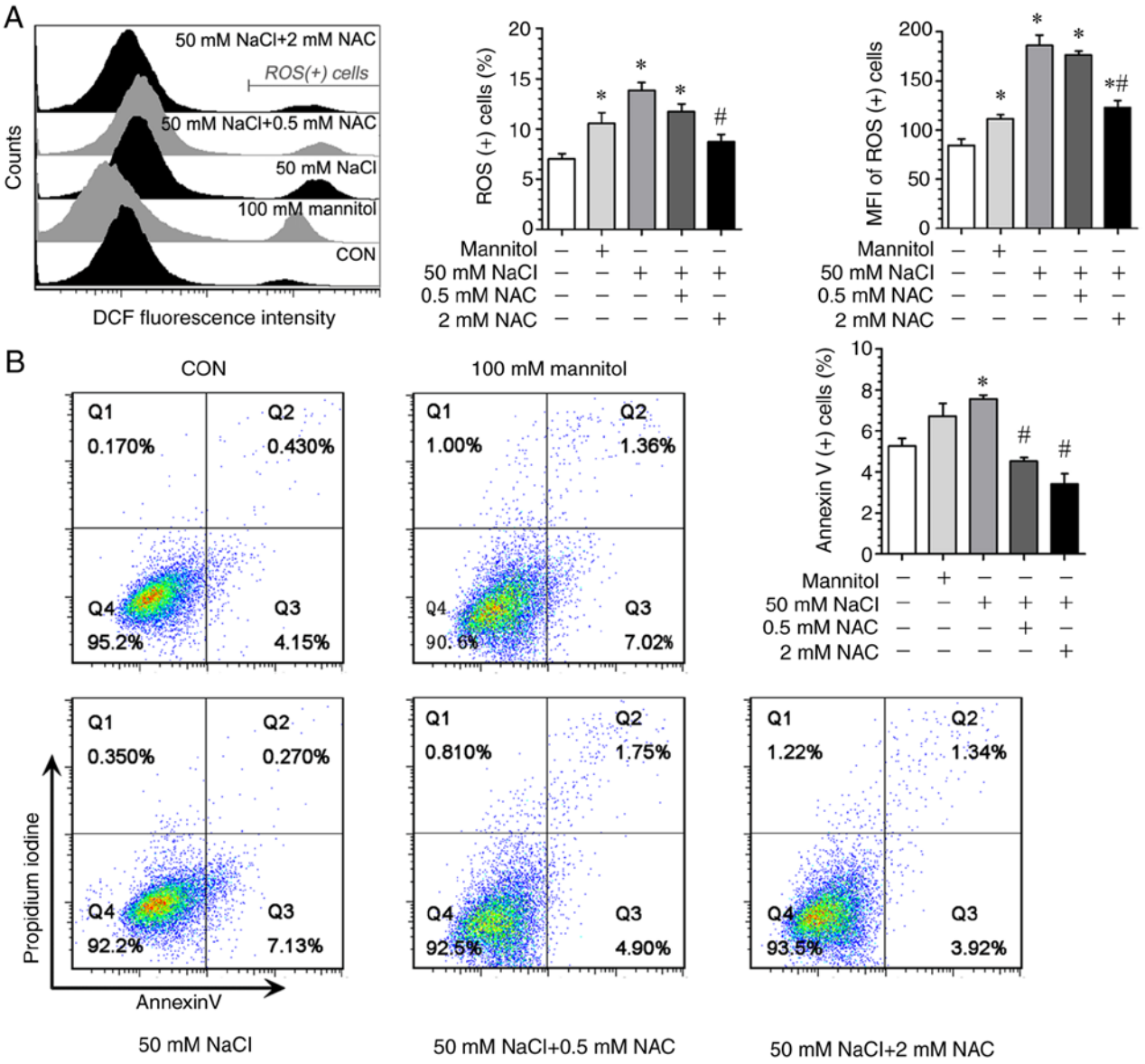

Figure 8. Increased extracellular [Na^+] contributes to enhanced ROS production and pro-apoptotic response in H9c2 cells. (A) Flow cytometric analysis of intracellular ROS production by 2,7-dichlorofluorescein diacetate in H9c2 cells. (B) Representative flow cytometric analysis (annexin V and propidium iodide double staining) of the H9c2 cardiac cells after treated with additional 50 mM NaCl in the culture medium for 24 h. The statistical analysis of present data is determined by one-way ANOVA followed by Newman-Keuls post hoc test. *P<0.05 vs. control and #P<0.05 vs. 50 mM NaCl. ROS, reactive oxygen species; NAC, N-acetylcysteine.

novel insights to elucidate their interactions. The first description of hypertension-related cardiac autophagy dates to a 1984 study, in which obvious autophagic vacuoles with lysosomal activity were observed in SHR over 20 months of age (29). The effectiveness of dietary intervention with different NaCl contents (0.5, 4.0 and 8%) in inducing LV dysfunction in SHR was previously compared systematically (12), since it is time consuming to induce hypertensive LV dysfunction in SHR [an overt cardiac dysfunction occurs at age of 52 to 90 weeks (30)]. It was revealed that 8 to 12 weeks after 8% salt-loading is the key time window in which a transition from compensated to decompensated LV hypertrophy occurs (12). Based on these findings, the dietary intervention was extended to 16 weeks and a global change of myocardial autophagy was demonstrated at 12 weeks after HS challenge, which persisted to 16 weeks. Notably, a temporal and spatial coincidence of progressive deterioration of LV systolic and diastolic dysfunction was also observed during this period. Therefore, the present study demonstrated the kinetics and association between autophagic change and LV remodeling in HS-diet-fed SHR. Notably, an overt LV dysfunction and the global activation of ATG components were not observed in the HS-fed WKY rats, indicating the inadequacy of stress severity (HS intake *per se*, without hemodynamic overload) and/or stress duration.

To explore the potential mechanism underlying the excessive change of myocardial autophagy, the hypothesis that chronic HS intake may lead to myocardial interstitial hyperosmolality was examined. The plasma [Na^+] is normally maintained within a narrow range by a rigorous control system. However, the results from previous studies (15,31,32), have expanded this concept by showing that chronic dietary high salt intake leads to Na^+ storage in the extracellular space

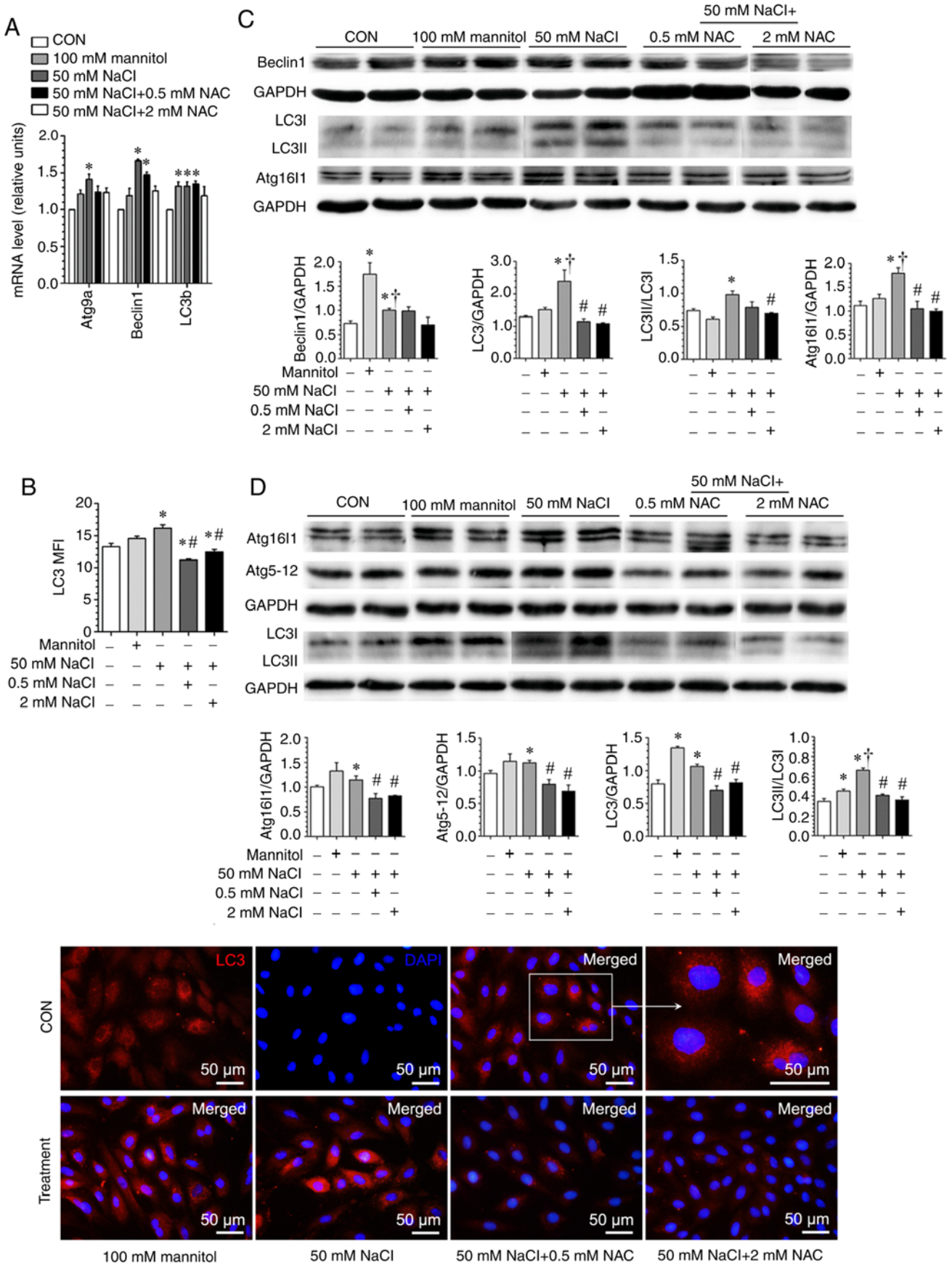

Figure 9. Na^+-leak induced cytosolic [Na^+] elevation contributes to reactive oxygen species-dependent autophagy activation and autophagosome formation in H9c2 cells. (A) Reverse transcription-quantitative PCR analysis of mRNA levels of autophagy genes. (B) Autophagosome immunofluorescent staining (LC3, rhodamine labeled, red) and related statistical comparisons. (C and D) Western blot analysis of autophagy-related proteins. The statistical analysis of present data is determined by one-way ANOVA followed by Newman-Keuls post hoc test. *P<0.05 vs. control, #P<0.05 vs. 50 mM NaCl and †P<0.05 vs. mannitol. The statistical results are derived from 4 to 5 independent tests. CON, control group (no additional NaCl); MFI, median fluorescence intensity; ATG, autophagy-related genes; LC3, light chain 3.

without a commensurate retention of water, which could yield a hypertonicity state in the interstitium. Additionally, in cartilage, the negative charge density of glycosaminoglycans contributes to the local interstitial [Na^+] at 450 mM, which far exceeds the serum [Na^+] (32). In the present study, using similar procedure, it was identified that myocardial interstitial [Na^+] is ~200 mM, and will be increased after chronic HS intake. Moreover, a proportional increase of cardiomyocyte TonEBP expression in response to hyperosmolality has been demonstrated previously (33). In the present study, using heart tissue ashing procedure, it was found that LV interstitial [Na^+] is over 200 mM, and will be increased after chronic HS intake. Moreover, TonEBP (or the nuclear factor of activated T cells 5, a well-characterized transcription factor induced by osmotic stress) expression was increased in HS-diet-fed rats, thus providing evidence supportive of myocardial interstitial hyperosmolality.

Next, it was examined whether increased extracellular [Na^+] may have a direct impact on myocardial autophagic change. Because the role of oxidative stress in regulating LV autophagic change is well characterized (34,35), the hypothesis that ROS generation may be the bridge linking extracellular hypertonicity and autophagic change was examined. A dose-dependent cytosolic [Na^+] elevation was revealed as extracellular [Na^+] increased, which induced the upregulation of key autophagy components at both the mRNA and protein levels in a ROS-dependent manner. A previous study revealed that in the failing heart, elevated cytosolic [Na^+] promotes ROS formation by reducing mitochondrial Ca^{2+} uptake via the Na^+/Ca^{2+} exchanger (36). Considering the close relationship between HS intake and myocardial oxidative stress (37), it is conceivable that this cytosolic [Na^+] elevation-triggered ROS production would work in tandem with hemodynamic stress in a vicious cycle to promote LV dysfunction. Because a variety of channels and/or exchangers, such as voltage-gated sodium channels and transient receptor potential channels (non-selective cation channels), are responsible for the transmembrane Na^+ influx, the precise mechanism for this 'Na^+ leak', when exposed to extracellular [Na^+] that is significantly elevated above the plasma level, remains to be elucidated in future studies.

Although autophagy is implicated as a key pathological event during hypertensive ventricular remodeling, to the best of our knowledge, our current understanding of myocardial autophagy in this setting is mainly derived from the LV pressure overloaded model (TAC in mice) (26). The reason may be ascribed to the time-consuming nature of *bone fide* hypertensive models, such as SHR. Though the LV autophagic change and its association with the hypertensive LV remodeling induced by chronic HS intake were observed in SHR, whether autophagy is upregulated in this pathophysiological process needs further studies to be confirmed.

In conclusion, the present study demonstrated that the myocardial autophagic change may participate in the maladaptive LV remodeling induced by chronic HS intake in SHR, and revealed a novel mechanism by which interstitial hypertonicity-induced cytosolic [Na^+] elevation triggers ROS-dependent autophagic change. The present results strengthen the notion that autophagy regulation may have therapeutic potential in cardiovascular disease, and provides a novel mechanism for HS intake-induced LV remodeling.

Acknowledgements

Not applicable.

Funding

The present study was supported by the National Natural Science Foundation of China (grant no. 81600328), the National Key R&D Program of China (grant nos. 2017YFC1307600 and 2017YFC1307602) and the Tianjin Municipal Science and Technology Committee (grant nos. 16JCQNJC11800, 15ZXJZSY00010 and 16ZXMJSY00130).

Availability of data and materials

The datasets used and/or analyzed during the present study are available from the corresponding author on reasonable request.

Authors' contributions

YB performed the experiments and wrote the manuscript. GHY conceptualized the study design and wrote the manuscript. SBC and WC analyzed the data and revised the manuscript. YB and ZZG performed the experiments and provided material support. XZ and YML conceptualized the study and interpreted the data, and confirm the authenticity of all the raw data. All authors have read and approved the final manuscript.

Ethics approval and consent to participate

All of the studies were performed in agreement with the national and international laws and policies and were approved by the Institutional Animal Care and Ethics Committee of Characteristic Medical Center of the Chinese People's Armed Police Forces (Tianjin, China; approval no. 2012-0005).

Patient consent for publication

Not applicable.

Competing interests

The authors declare that they have no competing interests.

References

1. Lee SS, McGrattan A, Soh YC, Alawad M, Su TT, Palanisamy UD, Hussin AM, Kassim ZB, Ghazali ANB, Stephan BC, *et al*: Feasibility and acceptability of a dietary intervention to reduce salt intake and increase high-nitrate vegetable consumption in malaysian middle-aged and older adults with elevated blood pressure: Findings from the DePEC-nutrition trial. Nutrients 14: 430, 2022.
2. Pires NM, Igreja B and Soares-da-Silva P: Antagonistic modulation of SIK1 and SIK2 isoforms in high blood pressure and cardiac hypertrophy triggered by high-salt intake. Clin Exp Hypertens 43: 428-435, 2021.
3. Hao J, Chang L, Wang D, Ji C, Zhang S, Hou Y and Wu Y: Periplocin alleviates cardiac remodeling in DOCA-salt-induced heart failure rats. J Cardiovasc Transl Res 26: 10.1007/s12265-022-10277-2, 2022.
4. Hsu A, Duan Q, McMahon S, Huang Y, Wood SA, Gray NS, Wang B, Bruneau BG and Haldar SM: Salt-inducible kinase 1 maintains HDAC7 stability to promote pathologic cardiac remodeling. J Clin Invest 130: 2966-2977, 2020.

5. Wang X, Zhang G, Dasgupta S, Niewold EL, Li C, Li Q, Luo X, Tan L, Ferdous A, Lorenzi PL, *et al*: ATF4 protects the heart from failure by antagonizing oxidative stress. Circ Res 131: 91-105, 2022.
6. Wang Y and Epelman S: Cardiac macrophages, reactive oxygen species, and development of left ventricular dysfunction. JACC Basic Transl Sci 2: 699-701, 2017.
7. Wen JJ, Porter C and Garg NJ: Inhibition of NFE2L2-antioxidant response element pathway by mitochondrial reactive oxygen species contributes to development of cardiomyopathy and left ventricular dysfunction in chagas disease. Antioxid Redox Signal 27: 550-566, 2017.
8. Klionsky DJ, Petroni G, Amaravadi RK, Baehrecke EH, Ballabio A, Boya P, Pedro JM, Cadwell K, Cecconi F, Choi AMK, *et al*: Autophagy in major human diseases. EMBO J 40: e108863, 2021.
9. Nishida K and Otsu K: Autophagy during cardiac remodeling. J Mol Cell Cardiol 95: 11-18, 2016.
10. Yang L, Gao JY, Ma J, Xu X, Wang Q, Xiong L, Yang J and Ren J: Cardiac-specific overexpression of metallothionein attenuates myocardial remodeling and contractile dysfunction in l-NAME-induced experimental hypertension: Role of autophagy regulation. Toxicol Lett 237: 121-132, 2015.
11. Li MH, Zhang YJ, Yu YH, Yang SH, Iqbal J, Mi QY, Li B, Wang ZM, Mao WX, Xie HG and Chen SL: Berberine improves pressure overload-induced cardiac hypertrophy and dysfunction through enhanced autophagy. Eur J Pharmacol 728: 67-76, 2014.
12. Yang GH, Zhou X, Ji WJ, Zeng S, Dong Y, Tian L, Bi Y, Guo ZZ, Gao F, Chen H, *et al*: Overexpression of VEGF-C attenuates chronic high salt intake-induced left ventricular maladaptive remodeling in spontaneously hypertensive rats. Am J Physiol Heart Circ Physiol 306: H598-H609, 2014.
13. Yang GH, Zhou X, Ji WJ, Liu JX, Sun J, Dong Y, Jiang TM and Li YM: VEGF-C-mediated cardiac lymphangiogenesis in high salt intake accelerated progression of left ventricular remodeling in spontaneously hypertensive rats. Clin Exp Hypertens 39: 740-747, 2017.
14. Ma Y, Shi L, Zhao K and Zheng C: lncRNA FR215775 regulates Th2 differentiation in murine allergic rhinitis. J Immunol Res 2022: 7783481, 2022.
15. Machnik A, Neuhofer W, Jantsch J, Dahlmann A, Tammela T, Machura K, Park JK, Beck FX, Müller DN, Derer W, *et al*: Macrophages regulate salt-dependent volume and blood pressure by a vascular endothelial growth factor-C-dependent buffering mechanism. Nat Med 15: 545-552, 2009.
16. Bortner CD, Sifre MI and Cidlowski JA: Cationic gradient reversal and cytoskeleton-independent volume regulatory pathways define an early stage of apoptosis. J Biol Chem 283: 7219-7229, 2008.
17. Livak KJ and Schmittgen TD: Analysis of relative gene expression data using real-time quantitative PCR and the 2(-Delta Delta C(T)) method. Methods 25: 402-408, 2001.
18. Kumar S, Javed R, Mudd M, Pallikkuth S, Lidke KA, Jain A, Tangavelou K, Gudmundsson SR, Ye C, Rusten TE, *et al*: Mammalian hybrid pre-autophagosomal structure HyPAS generates autophagosomes. Cell 184: 5950-5969 e5922, 2021.
19. Vigliano CA, Meckert PM, Diez M, Favaloro LE, Cortes C, Fazzi L, Favaloro RR and Laguens RP: Cardiomyocyte hypertrophy, oncosis, and autophagic vacuolization predict mortality in idiopathic dilated cardiomyopathy with advanced heart failure. J Am Coll Cardiol 57: 1523-1531, 2011.
20. Kim EJ, Choi MJ, Lee JH, Oh JE, Seo JW, Lee YK, Yoon JW, Kim HJ, Noh JW and Koo JR: Extracellular fluid/intracellular fluid volume ratio as a novel risk indicator for all-cause mortality and cardiovascular disease in hemodialysis patients. PLoS One 12: e0170272, 2017.
21. Wiig H, Luft FC and Titze JM: The interstitium conducts extrarenal storage of sodium and represents a third compartment essential for extracellular volume and blood pressure homeostasis. Acta Physiol (Oxf): Nov 28, 2018 (Epub ahead of print).
22. Lopes LR, Garcia-Hernandez S, Lorenzini M, Futema M, Chumakova O, Zateyshchikov D, Isidoro-Garcia M, Villacorta E, Escobar-Lopez L, Garcia-Pavia P, *et al*: Alpha-protein kinase 3 (ALPK3) truncating variants are a cause of autosomal dominant hypertrophic cardiomyopathy. Eur Heart J 42: 3063-3073, 2021.
23. Pitsch M, Kant S, Mytzka C, Leube RE and Krusche CA: Autophagy and endoplasmic reticulum stress during onset and progression of arrhythmogenic cardiomyopathy. Cells 11: 96, 2021.
24. Sun W, Lu H, Dong S, Li R, Chu Y, Wang N, Zhao Y, Zhang Y, Wang L, Sun L and Lu D: Beclin1 controls caspase-4 inflammsome activation and pyroptosis in mouse myocardial reperfusion-induced microvascular injury. Cell Commun Signal 19: 107, 2021.
25. Frustaci A, Letizia C, Chimenti C, Verardo R, Alfarano M, Scialla R, Bagnato G, Miraldi F, Sansone L and Russo MA: Myocardial aldosterone receptor and aquaporin 1 up-regulation is associated with cardiomyocyte remodeling in human heart failure. J Clin Med 10: 4854, 2021.
26. Wang ZV, Rothermel BA and Hill JA: Autophagy in hypertensive heart disease. J Biol Chem 285: 8509-8514, 2010.
27. Zhu H, Tannous P, Johnstone JL, Kong Y, Shelton JM, Richardson JA, Le V, Levine B, Rothermel BA and Hill JA: Cardiac autophagy is a maladaptive response to hemodynamic stress. J Clin Invest 117: 1782-1793, 2007.
28. Nakai A, Yamaguchi O, Takeda T, Higuchi Y, Hikoso S, Taniike M, Omiya S, Mizote I, Matsumura Y, Asahi M, *et al*: The role of autophagy in cardiomyocytes in the basal state and in response to hemodynamic stress. Nat Med 13: 619-624, 2007.
29. Tomanek RJ, Trout JJ and Lauva IK: Cytochemistry of myocardial structures related to degenerative processes in spontaneously hypertensive and normotensive rats. J Mol Cell Cardiol 16: 227-237, 1984.
30. Pfeffer JM, Pfeffer MA, Fishbein MC and Frohlich ED: Cardiac function and morphology with aging in the spontaneously hypertensive rat. Am J Physiol 237: H461-H468, 1979.
31. Schafflhuber M, Volpi N, Dahlmann A, Hilgers KF, Maccari F, Dietsch P, Wagner H, Luft FC, Eckardt KU and Titze J: Mobilization of osmotically inactive Na+ by growth and by dietary salt restriction in rats. Am J Physiol Renal Physiol 292: F1490-F1500, 2007.
32. Titze J and Machnik A: Sodium sensing in the interstitium and relationship to hypertension. Curr Opin Nephrol Hypertens 19: 385-392, 2010.
33. Navarro P, Chiong M, Volkwein K, Moraga F, Ocaranza MP, Jalil JE, Lim SW, Kim JA, Kwon HM and Lavandero S: Osmotically-induced genes are controlled by the transcription factor TonEBP in cultured cardiomyocytes. Biochem Biophys Res Commun 372: 326-330, 2008.
34. Ren J, Wu NN, Wang S, Sowers JR and Zhang Y: Obesity cardiomyopathy: Evidence, mechanisms, and therapeutic implications. Physiol Rev 101: 1745-1807, 2021.
35. Rabinovich-Nikitin I, Rasouli M, Reitz CJ, Posen I, Margulets V, Dhingra R, Khatua TN, Thliveris JA, Martino TA and Kirshenbaum LA: Mitochondrial autophagy and cell survival is regulated by the circadian clock gene in cardiac myocytes during ischemic stress. Autophagy 17: 3794-3812, 2021.
36. Kohlhaas M, Liu T, Knopp A, Zeller T, Ong MF, Bohm M, O'Rourke B and Maack C: Elevated cytosolic Na+ increases mitochondrial formation of reactive oxygen species in failing cardiac myocytes. Circulation 121: 1606-1613, 2010.
37. Huang P, Shen Z, Yu W, Huang Y, Tang C, Du J and Jin H: Hydrogen sulfide inhibits high-salt diet-induced myocardial oxidative stress and myocardial hypertrophy in dahl rats. Front Pharmacol 8: 128, 2017.